allowing this problem to be addressed. Thus the relative ease of reduction of **1**, its low electronic excitation energy, and the high-field ^{1}H NMR shifts of its peripheral protons are all consistent with its antiaromatic 12-π-electron count.

From a chemical point of view the most appealing evidence for the relative aromaticities of **1** and **2** is the degree of dissociation of the adducts **3** and **4**. Qualitatively, the 14-electron π-system of **2** is more resistant to olefin addition than is the 12-electron π-system of **1**. We can quantify this conclusion if we assume that the entropy changes associated with the two reactions are similar. The difference in the two equilibrium constants is then determined solely by ΔE_{deloc}, the delocalization energy change, for each reaction.[47] From the expression given in eq 6, the observed K_{diss}

$$-2.303RT \log \frac{K_{diss}(3,1)}{K_{diss}(4,2)} = \Delta E_{deloc}(3,1) - \Delta E_{deloc}(4,2) \quad (6)$$

values translate into a 5 kcal/mol difference in ΔE_{deloc} for the two reactions; i.e. **2** is more aromatic than **1** by 5 kcal/mol.

Just as benzene is more aromatic (more resistant to Diels–Alder addition) than naphthalene,[47] so too is trithiadiazepine itself relative to benzotrithiadiazepine. The former fails to react at all with olefins and undergoes electrophilic substitution typical of a benzenoid aromatic compound.[12]

Acknowledgment. We thank the Natural Sciences and Engineering Research Council of Canada, the Research Corp., the National Science Foundation (EPSCOR Grant ISP 801147), and the State of Arkansas for financial support of this work. We also thank Dr. J. F. Richardson for collecting a low-temperature X-ray data set on **1**.

Registry No. **1**, 34357-13-6; **2**, 97484-08-7; **3**, 100765-34-2; **4**, 100765-35-3; **5**, 22706-22-5; **6**, 273-77-8; PhN=S=NSiMe$_3$, 56839-46-4; Me$_3$SiNHPh, 3768-55-6; Me$_3$SiN=S=O, 7522-26-1; SCl_2, 10545-99-0; 2-ClSC$_6$H$_4$SCl, 30818-49-6; Me$_3$SiN=S=NSiMe$_3$, 88266-99-3; norbornadiene, 121-46-0.

Supplementary Material Available: Listings of anisotropic thermal parameters for **1** (Table S1), **3** (Table S2), and **4** (Table S3) and structure factors for each structure (44 pages). Ordering information is given on any current masthead page.

(47) Dewar, M. J. S. "The Molecular Orbital Theory of Organic Chemistry"; McGraw-Hill: New York, 1969.

Contribution from the Department of Chemistry, Victoria University of Wellington, Wellington, New Zealand, and Christopher Ingold Laboratories, University College London, London WC1H 0AJ, United Kingdom

Raman and Resonance Raman Studies of Tetraphosphorus Triselenide

Gary R. Burns,*† Joanne R. Rollo,† and Robin J. H. Clark*‡

Received August 8, 1985

The first-order Raman-active phonons of P_4Se_3 have been found to be resonance-enhanced. The Raman band excitation profiles measured at 295 K show broad maxima at 14 400 cm^{-1}, red shifted by 4500 cm^{-1} with respect to the absorption edge and by 11 500 cm^{-1} with respect to the electronic band maximum in solution. A recent redetermination of the crystal structure at 265 K has identified significant selenium–selenium intermolecular contacts that produce a layer lattice in which helical chains of P_4Se_3 molecules are directed along the unit cell *a* and *b* axes. It is proposed that the layer lattice confers semiconducting properties on crystalline P_4Se_3 and that the resulting anisotropic resonant transition may be the cause of the enhancement of the Raman-active phonons.

Introduction

The molecules P_4S_3, P_4Se_3, As_4S_3, and As_4Se_3 are the simplest structures found among the large number of cage molecules formed by phosphorus and arsenic with the chalcogen elements sulfur and selenium. Interest in this group of compounds has been stimulated by the growing importance of chalcogenide glasses in current technology.[1] Amorphous chalcogenides are used in fast electrical switches, computer memories, display devices, and television cameras. It is also possible that amorphous films of chalcogenide glasses may be used in the manufacture of layered acoustic wave guides and in the storage of holograms.

P_4S_3 and P_4Se_3 occur as crystalline (α) and plastic (β) modifications, where the latter is characterized by an ordered arrangement of molecules on a lattice but with a high degree of orientational disorder. In this work we shall be mainly concerned with the low-temperature crystalline phase but will make some use of Raman data for the β-phase.

Despite the apparent simplicity of the parent C_{3v} cage (see Figure 1) there is no complete and unambiguous assignment of the normal modes for any of these molecules. Numerous spectroscopic studies[2-6] and a number of normal coordinate treatments[7-11] have failed to characterize the $4a_1 + a_2 + 5e$ normal modes.

The P_4S_3 molecule has received the greatest attention, and there is now a considerable body of information on its Raman- and infrared-active vibrations. These studies have been aided by the high solubility of P_4S_3 in carbon disulfide and by the greater relative stability of P_4S_3 compared to P_4Se_3 in all phases.

The purposes of this study were to investigate the low-temperature (80 K) Raman spectrum of P_4Se_3 in an attempt to resolve the crystal field and Davydov components of the a_1 and e molecular modes, and to see whether there was any resonance enhancement of the Raman-active vibrations for excitation within the contour of the low-energy absorption band. A toluene solution of P_4Se_3 has an electronic absorption band with a maximum at 387 nm

†Victoria University of Wellington.
‡University College London.

(1) Davis, E. A. *Endeavour* **1977**, *1*, 103.
(2) Bues, W.; Somer, M.; Brockner, W. *Z. Naturforsch., B: Anorg. Chem., Org. Chem.* **1980**, *35B*, 1063 and earlier references therein.
(3) Chattopadhyay, T.; Carlone, C.; Jayaraman, A.; von Schnering, H. G. *Phys. Rev. B: Condens. Matter* **1981**, *23*, 2471.
(4) Chattopadhyay, T.; von Schnering, H. G. *Phys. Status Solidi B* **1981**, *103*, 637.
(5) Chattopadhyay, T.; von Schnering, H. G. *Phys. Status Solidi B* **1981**, *108*, 241.
(6) Chattopadhyay, T.; Carlone, C.; Jayaraman, A.; von Schnering, H. G. *J. Phys. Chem. Solids* **1982**, *43*, 277.
(7) Gerding, H.; Marsden, J. W.; Nobel, P. C. *Recl. Trav. Chim. Pays-Bas* **1957**, *76*, 757.
(8) Cyvin, S. J.; Brunvoll, J.; Cyvin, B. N.; Somer, M.; Brockner, W. *Z Naturforsch., A: Phys., Phys. Chem., Kosmophys.* **1980**, *35A*, 1062.
(9) Cyvin, S. J.; Cyvin, B. N.; Somer, M.; Brockner, W. *J. Naturforsch., A: Phys., Phys. Chem., Kosmophys.* **1981**, *36A*, 774.
(10) Brockner, W.; Somer, M.; Cyvin, B. N.; Cyvin, S. J. *Z. Naturforsch., A: Phys., Phys. Chem., Kosmophys.* **1981**, *36A*, 846.
(11) Brunvoll, J.; Cyvin, B. N.; Cyvin, S. J. *Z. Naturforsch., A: Phys., Phys. Chem., Kosmophys.* **1982**, *37A*, 342.

0020-1669/86/1325-1145$01.50/0

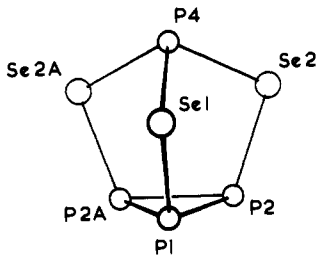

Figure 1. The cagelike molecule P_4Se_3.

(ϵ = 268 M^{-1} cm^{-1}) but the maximum possible concentration is too low to permit Raman measurements to be made. Exploratory Raman studies of crystalline P_4Se_3 showed that, rather than displaying maximum intensity for blue excitation, P_4Se_3 has strongly resonance-enhanced Raman-active phonons for red excitation.

Measurement of the reflectance spectrum of P_4Se_3, as a polycrystalline powder, showed that the electronic absorption band maximum is strongly red-shifted, clearly indicating the presence of strong intermolecular lattice forces. Confirmation of strong intermolecular bonding could not be obtained from the original X-ray data[12] but has recently been established on the basis of a redetermination of the X-ray crystal structure of α-P_4Se_3 (vide infra).

Experimental Details

P_4Se_3 was prepared by refluxing a mixture of yellow phosphorus dissolved in *n*-heptane and selenium in the presence of a charcoal catalyst.[13] The product was purified by Soxhlet extraction using benzene as the solvent, followed by recrystallization from carbon disulfide under an atmosphere of nitrogen.

For Raman measurements at room temperature, solid samples were dispersed in $K[NO_3]$ and rotated at ca. 1000 rpm. The sample as a microcrystalline powder was pressed over one-half of the circumference of a rotating disk, the internal standard occupying the other half. This technique is similar to the divided disk method of Machida and Tsukamoto[14] and shows the same advantage in signal intensity for the reference. Low-temperature Raman measurements were obtained for pressed disks of P_4Se_3 dispersed in $K[NO_3]$ and mounted on a copper block in a liquid-nitrogen-cooled Dewar.

Raman spectra were recorded with Spex 1401 and 14018 double monochromators in conjunction with a Spectra Physics Model 164-01 krypton ion laser, Coherent Radiation Models CR12 argon ion and CR500K krypton ion lasers, and a Model CR490 dye laser using rhodamine 6G. Laser excitation ranging from 350.7 to 799.3 nm was used with power at the sample restricted to $\leq$50 mW so as to avoid thermal decomposition of the sample.

Detection of the scattered radiation was by standard photon-counting techniques employing RCA C31034 photomultipliers. Wavenumber measurements were calibrated by reference to the emission spectrum of neon, and band intensities were corrected for the spectral response of the spectrometers.

Electronic absorption spectra were recorded for a toluene solution of P_4Se_3 in a quartz cuvette cell, for a solid sample dispersed in a KBr pressed disk, and for a sample dissolved in Dow Corning 210 silicone oil (dimethyl polysiloxane). Silicone oil acts as a matrix into which the sample may be introduced by first dissolving the sample and the oil in a hydrocarbon solvent. The solvent is then removed by pumping under vacuum to leave an extremely viscous and concentrated solution. The diffuse reflectance spectrum of microcrystalline P_4Se_3 was recorded by using a Unicam SP700 spectrophotometer.

Raman polarization data could not be obtained for P_4Se_3 in solution. In the case of organic solvents (toluene, carbon disulfide, etc.) the concentration was too low, even on being warmed in a sealed tube; in the case of the silicone oil solution, rapid decomposition took place in the laser beam.

The infrared spectrum of P_4Se_3 was obtained on a Perkin-Elmer 599B infrared spectrophotometer. The sample, as a polycrystalline film prepared from a benzene solution of P_4Se_3, was held on a cesium bromide plate. The plate was mounted in a copper block attached to a Dewar flask cooled by liquid nitrogen.

(12) Keulen, E.; Vos, A., *Acta Crystallogr.* **1959**, *12*, 323.
(13) Irgolic, K.; Zingaro, R.; Kudchadker, M. *Inorg. Chem.* **1965**, *4*, 1421.
(14) Machida, K.; Tsukamoto, I. *J. Raman Spectrosc.* **1984**, *15*, 169.

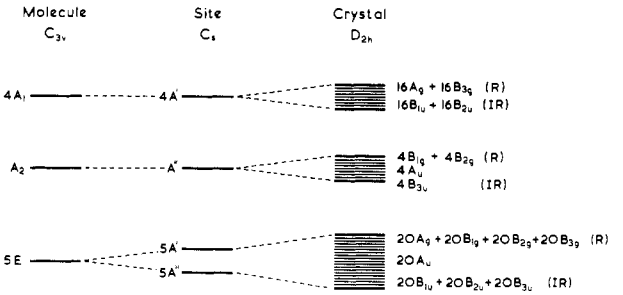

Figure 2. Correlation diagram for the 15 internal modes of vibration of α-P_4Se_3 with the 240 factor group components of the molecule (D_{2h}^{16}) unit cell.

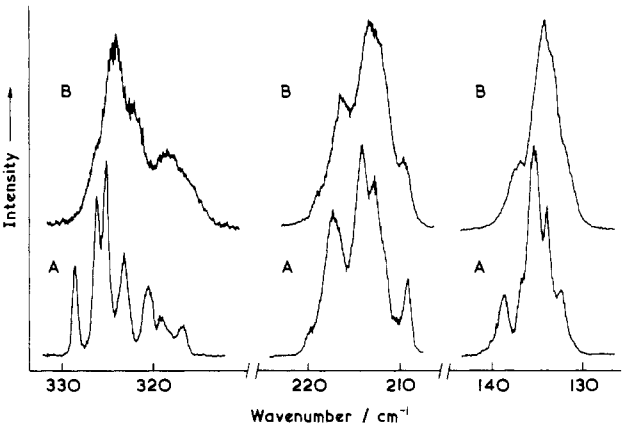

Figure 3. 135-, 213-, and 324-cm^{-1} Raman-active bands of α-P_4Se_3 measured at 80 (A) and 295 K (B) with an instrument slit width of 0.46 cm^{-1}. The sample was illuminated with 10 mW of 676.4-nm radiation.

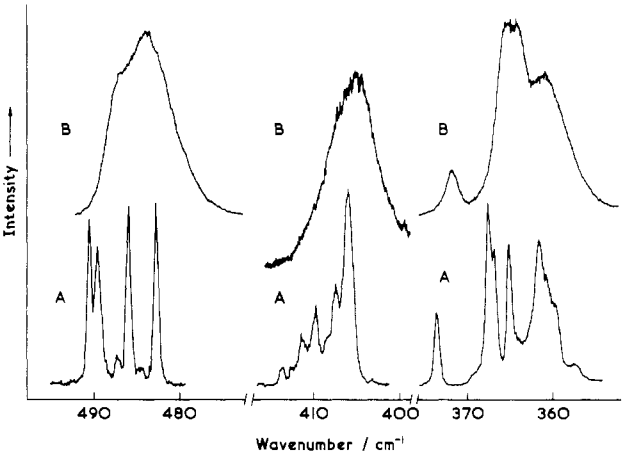

Figure 4. 365-, 405-, and 484-cm^{-1} Raman-active bands of α-P_4Se_3 measured at 80 (A) and 295 K (B) with an instrument slit width of 0.46 cm^{-1}. The sample was illuminated with 10 mW of 676.4-nm radiation.

Results

Raman Spectra. P_4Se_3 crystallizes in the space group *Pnma* (D_{2h}^{16}) with 16 molecules in the unit cell and with each molecule occupying a site of C_s symmetry. The correlation diagram (see Figure 2) shows that each a_1 internal mode gives rise to $4a_g$ + $4b_{3g}$ Raman-active phonons and $4b_{1u}$ + $4b_{2u}$ infrared-active phonons. The a_2 internal mode, forbidden in both the infrared and Raman spectra for the free molecule, gives rise to $4b_{1g}$ + $4b_{2g}$ Raman-active phonons and $4b_{3u}$ infrared-active phonons. Each e internal mode gives rise to $4a_g$ + $4b_{1g}$ + $4b_{2g}$ + $4b_{3g}$ Raman-active phonons and $4b_{1u}$ + $4b_{2u}$ + $4b_{3u}$ infrared-active phonons.

The six structured Raman bands of crystalline P_4Se_3 at 295 and 80 K are shown in Figures 3 and 4, and the phonon wavenumbers are given in Table I. The number of Raman-active phonons observed is many fewer than is predicted. This is to be

Table I. Raman Bands Observed for Crystalline α-P_4Se_3

ref 2	this work		
293 K	295 K	80 K	assignts
	132.1	132.5	
	133.7	134.2	
132	134.5	135.5	e
	...	136.8	
	137.3	138.7	
	209.4	209.0	
	...	212.6	
207	213.0	213.8	a_1
211	216.0	217.1	
	218.8	219.8	
	315.6	316.6	
315	318.1	318.6	e
	...	320.4	
	321.9	323.0	
320	323.9	325.0	
	...	326.0	a_1
	326	328.4	
344	...	357.3	
	...	359.6	
356	361.0	361.3	e
360	364.8	364.9	
	...	366.8	
	...	367.3	
	...	369.0	a_1
369	371.8	373.6	
404	404.8	405.8	
		407.3	
		409.7	e
		411.3	
		413.6	
		482.5	
	483.8	484.3	
485		485.7	
	486.4	487.0	a_1
		489.2	
		490.3	

expected, since some of the Davydov splittings are probably too small to be resolved. Even if all the Davydov splittings were large, the isotope-based broadening of the phonon bands would prevent their resolution.

A total of $4a_1 + 5e$ internal modes of the isolated molecule should be observable in the Raman spectrum, with the a_2 mode possibly appearing with very low intensity in the crystal. It has not been possible to grow sufficiently large pure crystals of P_4Se_3 suitable to measure the polarization of the Raman-active phonons. Bues et al.[2] have obtained polarization data for a β-P_4Se_3 melt at 300 °C, which identifies bands at 486, 373, 323, and 220 cm^{-1} as arising from the four a_1 modes and bands at 140, 160, 352, and 408 cm^{-1} as arising from e modes. They assign the weak shoulder at 315 cm^{-1} in their 293 K Raman spectrum of α-P_4Se_3 to the remaining e mode.

We have not observed any feature analogous to the 160-cm^{-1} band of β-P_4Se_3 in the 80 K spectrum of α-P_4Se_3. However, we agree with Bues et al. that two of the e modes are likely to be the Raman-active phonons giving rise to the low-energy wings of the Raman bands centered at 323.9 and 364.8 cm^{-1} at 295 K. Additional support for these assignments comes from the infrared spectrum for a polycrystalline film of α-P_4Se_3 (see Figure 5). The two bands at 310 and 350 cm^{-1} at 295 K shift to 312 and 352 cm^{-1} at 80 K with the appearance of shoulders at 317, 334, and 362 cm^{-1}.

The other notable feature of the 80 K Raman spectrum of α-P_4Se_3 is the large Davydov splitting observed for most bands by comparison to that observed for either P_4S_3[3] or As_4S_3.[6] This presumably reflects the strong intermolecular coupling present in α-P_4Se_3.

Attempts to calculate the wavenumbers of the P_4Se_3 modes on the basis of assignments for P_4S_3 are frustrated by the absence of any obvious scaling relation between the two molecules and

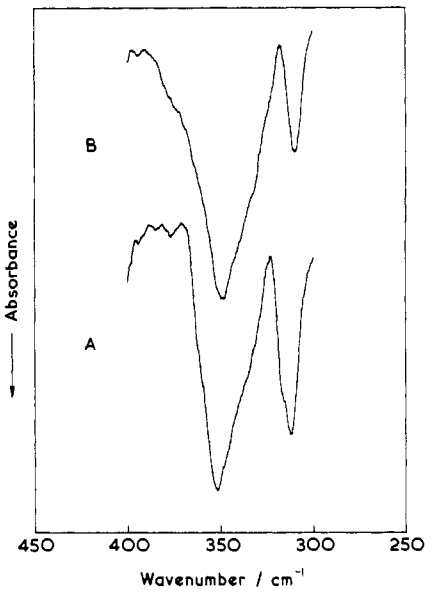

Figure 5. Infrared absorption spectrum of a polycrystalline sample of α-P_4Se_3 measured at ca. 80 (A) and ca. 295 K (B).

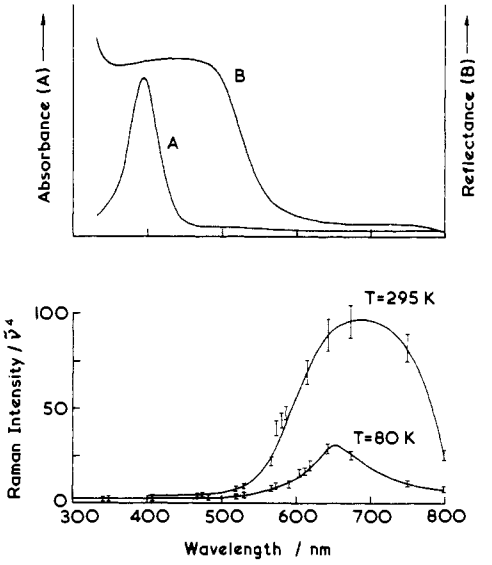

Figure 6. Excitation profiles for the 365-cm^{-1} band of α-P_4Se_3 measured at 80 and 295 K together with the electronic absorption spectrum of a toluene solution (A) and the diffuse-reflectance spectrum of α-P_4Se_3 (B).

by uncertainties over the assignments for P_4S_3. Hence the best assignments to date are shown in Table I, based largely on polarization data for molten P_4Se_3 together with infrared and Raman data for α-P_4Se_3.

Resonance Raman Spectra and Excitation Profiles. By using the ν_1 band of $K[NO_3]$ as an internal intensity standard, we have constructed excitation profiles for the 365-cm^{-1} band of P_4Se_3 at 295 K and at 80 K. The intensity measurements were taken for both the 364.8- and the 371.8-cm^{-1} components at 295 K, but it was found that for each exciting line the ratio of the intensities of the two was the same, the 364.8-cm^{-1} component being 13 times more intense than that at 371.8 cm^{-1}. The 80 K intensity data were measured by using the 361.0- and 373.6-cm^{-1} components. For each exciting line the ratio of the intensities was the same, the 361.0-cm^{-1} component being 16 times more intense than that at 373.6 cm^{-1}.

The different choice of component for the pressed disk of P_4Se_3 at 80 K was due to a pressure-induced change in the 365-cm^{-1} band contour.

In both excitation profiles a maximum occurs well into the red compared to the absorption edge of crystalline P_4Se_3 and the electronic absorption maximum for a toluene solution of P_4Se_3

(see Figure 6). The 80 K excitation profile has a broad maximum at 655 nm, which shifts to 695 nm at 295 K. Excitation profiles for bands at 484, 324, 213, and 135 cm^{-1} show the same maxima as for the 365-cm^{-1} band. The band at 405 cm^{-1} is too weak to give reliable intensity data.

The absence of any overtone progression together with the large red shift for the maximum in the excitation profile of P_4Se_3 with respect to the electronic absorption band maximum in solution and the absorption edge for the solid-state reflectance spectrum of crystalline P_4Se_3 is similar to the behavior observed for $Ag_2[CrO_4]$.[15]

It has been proposed that the intramolecular $^1T_2 \leftarrow {}^1A_1$ electronic band, localized on the $[CrO_4]^{2-}$ ion in alkali-metal chromates, is dispersed over the Brillouin zone in $Ag_2[CrO_4]$. Covalent interactions between silver ions and between silver and oxygen may confer on $Ag_2[CrO_4]$ the properties of a semiconductor. Robbins and Day[16] attribute the large red shift of the $^1T_2 \leftarrow {}^1A_1$ transition in $Ag_2[CrO_4]$ to a coupling of two intramolecular transitions whereby one is raised in energy and the other ($^1T_2 \leftarrow {}^1A_1$) is lowered in energy.

We favor a similar explanation for the red shift of the 387-nm absorption band of a solution of P_4Se_3 in going to the crystalline state. The nature of the electronic transition is not certain. There have been detailed SCFMO calculations[17,18] for the related molecule P_4S_3 for which the lowest energy electronic transitions are identified as $4a_2 \leftarrow$ 17e, 18e $\leftarrow$ 17e, $18a_1 \leftarrow$ 17e, and $19a_1 \leftarrow$ 17e, where the highest occupied molecular orbital (HOMO), 17e, is centered on the basal phosphorus atoms.

For P_4Se_3, the photoelectron spectrum[19] indicates that the HOMO is a selenium-based lone pair and therefore the visible band at 387 nm has an origin different from that of the lowest energy band in the electronic absorption spectrum of P_4S_3.

We can be reasonably confident that for P_4Se_3 the 387-nm band involves a transition where the ground state has a major contribution from the lone-pair electrons on the selenium atoms. The large red shift on going from the solution to the crystalline state implies some form of covalent intermolecular bonding involving selenium atoms of adjacent P_4Se_3 molecules. The original crystal structure data suggest that there may be significant Se···Se and P···Se interactions, but the structure was determined for only two projections. To obtain more accurate intermolecular bond lengths, the crystal structure of P_4Se_3 was redetermined[20] and a summary of the detail relevant to this work is given in the next section.

Comments on the X-ray Crystal Structure. The essential features of the Keulen and Vos structure[12] were confirmed by the redetermination[20] of the crystal structure at 265 K, but with an improved R factor of 4.28% and therefore a smaller uncertainty associated with the atom coordinates.

P_4Se_3 belongs to the orthorhombic primitive crystal system with space group *Pnma* (D_{2h}^{16}). There are four independent molecules per asymmetric unit and 16 molecules per unit cell.

One of the mirror planes of a P_4Se_3 molecule coincides with a mirror plane of the crystal, and the atoms Se1, P1, and P4 lie on the mirror planes at y = $^1/_4$, $^3/_4$ in the special fourfold sets of positions (c) of the space group *Pnma*. The remaining four atoms of the molecule occupy the general eightfold positions (d).

The average intramolecular bond lengths are 222.6 pm for P–P, 224.1 pm for P–Se, and 342.2 pm for Se–Se. Of more interest are the intermolecular distances, in particular those between selenium atoms. As shown in Figure 7, there are four unique intermolecular selenium–selenium contacts per unit cell ranging from 362.5 (6) to 379.8 (6) pm. The Pauling–van der Waals radius for selenium is 200 pm so that contact distances of 380 pm or less suggest that there is an interaction between selenium atoms stronger than a van der Waals interaction. The geometry of the intermolecularly bonded molecules is interesting in that helices directed along the *a* and *b* cell axes are similar to the helical chain configuration found for trigonal selenium.[21] The structure is best described in terms of a layer lattice with four layers per unit cell lying orthogonal to the *c* axis. Each layer consists of the helical chains of P_4Se_3 molecules directed along the *a* and *b* axes.

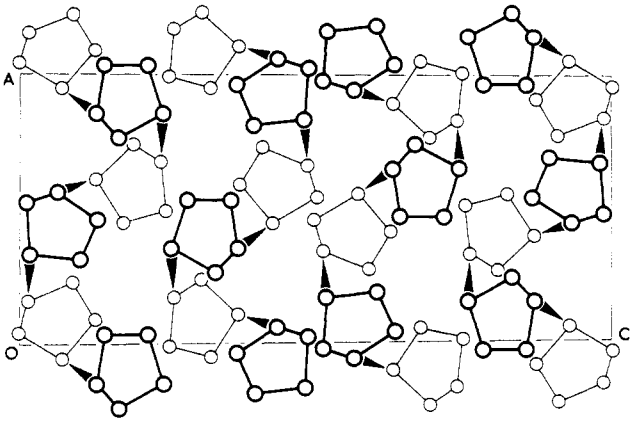

Figure 7. Projection of the structure of α-P_4Se_3 along the [010] direction. The four close Se···Se intermolecular contacts produce helical chains of P_4Se_3 molecules directed along the *a* and *b* unit cell axes. Molecules lying with their planes of symmetry at $y = {}^1/_4$ are shown in light type while those with their planes of symmetry at $y = {}^3/_4$ are shown in heavy type.

Between adjacent layers, contact distances of 365.3 and 373.2 pm between the phosphorus and selenium atoms may signify stronger than expected van der Waals interactions. The sum of the Pauling–van der Waals radii for phosphorus and selenium is 390 pm. However, that this distance is comparable to the Se–Se distance in the chains emphasises the greater importance of the Se–Se intermolecular interactions.

Discussion

The lowest energy electronic transition of molecular P_4Se_3 in solution is found to undergo a large red shift in the crystalline state. The absorption edge for polycrystalline P_4Se_3 at room temperature is at 530 nm. This is a red shift of 7000 cm^{-1} with respect to the absorption maximum at 387 nm for a toluene solution.

The Raman-active phonons of crystalline P_4Se_3 have been shown to be resonance-enhanced, with a maximum in the excitation profile for a sample at 295 K at 695 nm. This is a shift to the low-energy side of the room-temperature absorption edge of 4500 cm^{-1}. For a sample dispersed in $K[NO_3]$, the maximum in the excitation profile is at 655 nm, a shift of 3600 cm^{-1} to the low-energy side of the room-temperature absorption edge.

By analogy with $Ag_2[CrO_4]$, the observed red shift of the lowest energy electronic absorption band of P_4Se_3 on going from the molecular state in solution to the crystalline state and the enhancement of the Raman-active phonons can both be attributed to the presence of strong intermolecular bonding in the solid. It is proposed that the lowest energy electronic transition thereby acquires significant anisotropy and semiconductor character. The excitation profiles of the Raman-active phonons of P_4Se_3 show a maximum to the low-energy side of the resonant transition, presumably at a wavenumber that coincides with that of the imaginary part of the dielectric constant (ϵ'') which is related to the gap frequency, ω_g, of a semiconductor.[22]

The blue shift in the maximum of the excitation profile on going from 295 to 80 K may reflect a similar shift in the absorption edge. This would be a shift comparable to that observed for the layer lattice semiconductor As_2Se_3.[23]

(15) Clark, R. J. H.; Dines, T. J. *Inorg. Chem.* **1982**, *21*, 3585.
(16) Robbins, D. J.; Day, P. *Mol. Phys.* **1977**, *34*, 893.
(17) Head, J. D.; Mitchell, K. A. R.; Noodleman, L.; Paddock, N. L. *Can. J. Chem.* **1977**, *55*, 669.
(18) Palmer, M. H.; Findlay, R. H. *Z. Naturforsch., A: Phys., Phys. Chem., Kosmophys.* **1983**, *38A*, 78.
(19) Cannington, P. H.; Whitfield, H. J. *J. Electron Spectrosc. Relat. Phenom.* **1977**, *10*, 35.
(20) Burns, G. R.; Clark, R. J. H.; Dawes, H. M.; Hursthouse, M. B. *Acta Crystallogr.*, in press.
(21) Unger, P.; Cherin, P. In "Physics of Selenium and Tellurium"; edited by Cooper, W. C., Ed.; Pergamon: Oxford, England, 1969; p 223.
(22) Clark, R. J. H.; Kurmoo, M. *Inorg. Chem.* **1980**, *19*, 3522.

Strong intermolecular interactions between selenium atoms of adjacent P_4Se_3 molecules are implied by the results of a recent redetermination of the X-ray structure of P_4Se_3. The selenium–selenium interactions produce helical chains of P_4Se_3 molecules directed along the unit cell *a* and *b* axes. There are four layers containing *a*- and *b*-directed helical chains per unit cell. This structure has certain similarities with the helical chain configuration found for trigonal selenium and may explain why P_4Se_3 decomposes slowly to form red amorphous selenium.

Acknowledgment. G.R.B. is grateful to the Council of Victoria University of Wellington for granting a sabbatical leave, held at University College London, during which much of this work was completed.

Registry No. P_4Se_3, 1314-86-9.

(23) Zallen, R.; Slade, M. L. *Phys. Rev. B: Solid State* **1974**, *B9*, 1627.

Contribution from the Department of Chemistry, Louisiana State University, Baton Rouge, Louisiana 70803-1804

X-ray Single-Crystal Structure Determination of Copper(II), Cobalt(II), and Nickel(II) Complexes of 2,2-Bis(2-pyridyl)- and 2,2-Bis(6-methyl-2-pyridyl)-1,3-dioxolane[1]

George R. Newkome,* Hellen C. R. Taylor, Frank R. Fronczek, and Vinod K. Gupta

Received June 26, 1985

2,2-Bis(2-pyridyl)- and 2,2-bis(6-methyl-2-pyridyl)-1,3-dioxolane readily formed chelates with Co(II), Ni(II), and Cu(II). X-ray analysis of the Cu(II) and Co(II) complexes showed primary N-chelation through the pyridines with a moderate interaction to one of the dioxolane oxygens. In the octahedral Ni(II) complex of the methylpyridyl ketal, the ligand was bound to the metal in a tridentate fashion. $CuCl_2C_{13}H_{12}N_2O_2$ (**4**) is monoclinic, $P2_1/c$, a = 9.022 (2) Å, b = 12.053 (3) Å, c = 13.564 (5) Å, β = 108.50 (3)°, Z = 4, and R = 0.029 for 3107 observations. $CuCl_2C_{15}H_{16}N_2O_2$ (**5**) is triclinic, $P\bar{1}$, a = 8.221 (3) Å, b = 9.265 (4) Å, c = 11.351 (3) Å, α = 99.89 (3)°, β = 100.21 (3)°, γ = 100.08 (3)°, Z = 2, and R = 0.035 for 2267 observations. $CoCl_2C_{15}H_{16}N_2O_2$ (**7**) is monoclinic, $P2_1/n$, a = 8.658 (1) Å, b = 11.127 (4) Å, c = 16.731 (4) Å, β = 90.28 (2)°, Z = 4, and R = 0.036 for 2233 observations. $[Ni(C_{15}H_{16}N_2O_2)(H_2O)_3]Cl_2$ (**10**) is orthorhombic, *Pbca*, a = 12.185 (4) Å, b = 13.820 (5) Å, c = 21.881 (4) Å, Z = 8, and R = 0.033 for 2423 observations.

Introduction

Bidentate bis(2-pyridyl) ketone (**1**) can exhibit two modes of coordination: N,O-coordination generating a five-membered chelate ring and N,N-coordination (six-membered chelate), which are easily differentiated by the magnitude of the carbonyl stretching frequency [ν(CO)] in the IR spectrum.[2] In the free

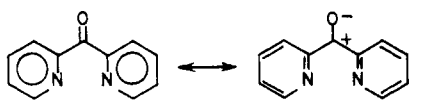

1a **1b**

ligand, the electron-poor nature of the pyridines reduces the carbonyl bond order, as evidenced by the comparatively low ν(CO) in **1b**: 1675 cm^{-1}.[3] O-Coordination should further diminish ν(CO), whereas N,N-coordination should increase the carbonyl bond order relative to **1**, and a shift ν(CO) to higher frequencies should be observed.

Osborne and McWhinnie reported[2] the first preparation of Cu(II) complexes of **1** and attributed changes in ν(CO) to an alteration in the mode of complexation from N,O to N,N. Several transition-metal [Mn(II), Fe(II), Co(II), Cu(II), and Ni(II)] complexes with **1** have been prepared and were proposed to be N,N-chelated on the basis of numerous similarities observed in the IR spectra of $[M(\mathbf{1})X_2]$.[3] It has been also reported[2] that water adds across the ketone of N,N-coordinated **1** to afforded stable *gem*-diols. Further studies[4,5] have demonstrated that nucleophiles add after the formation of the N,N-coordinated complex and that the serendipitous disposition of X provides the possibility of tridentate chelation by carbonyl adducts of **1**[6] (Figure 1).

More recent examples of **1** with U(IV),[7] Zn(II), Cd(II), and Hg(II),[8] and lanthanides [as Ln(III)][9] have been reported. In its hydrated form, **1** forms a (μ-peroxo)dicobalt(III) complex,[10] $[Co_2(\mathbf{1}\cdot H_2O)_4(py)_2O_2](ClO_4)_4$, upon oxygenation of the corresponding Co(II) complex. The Pd(II), Pt(II), and Au(III) chlorides also react with **1** to give complexes in which one or two ligand molecules, either the carbonyl or the *gem*-diol form, are coordinated to the metal ion.[11]

Numerous transition-metal complexes of **1** display a proclivity for nucleophilic addition to a carbonyl group as well as the stability of the "hydrate" complexes that result. Since both 2,2-bis(2-pyridyl)-1,3-dioxolane (**2**) and 2,2-bis(6-methyl-2-pyridyl)-1,3-dioxolane (**3**) possess a spiroketal function that can mimic the

2 **3**

"hydrated" form of **1**, we investigated the complexation properties of these ligands with Co(II), Ni(II), and Cu(II). In our earlier work we reported a novel series of (malonate ester-*C*)palladium complexes of **2** and conducted structural analysis to provide a

(1) Chemistry of Heterocyclic Compounds. 117. Part 116: Fronczek, F. R.; Taylor, H. C. R.; Gupta, V. K.; Newkome, G. R. *Acta Crystallogr., Sect. C: Cryst. Struct. Commun.* **1985**, *C41*, 1548.
(2) Osborne, R. R.; McWhinnie, W. R. *J. Chem. Soc. A* **1967**, 2075.
(3) Feller, M. C.; Robson, R. *Aust. J. Chem.* **1968**, *21*, 2919.
(4) Feller, M. C.; Robson, R. *Aust. J. Chem.* **1970**, *23*, 1997.
(5) Bakker, I. J.; Feller, M. C.; Robson, R. *J. Inorg. Nucl. Chem.* **1971**, *33*, 747.
(6) Fischer, B. E.; Sigel, H. *J. Inorg. Nucl. Chem.* **1975**, *37*, 2127.
(7) Ortego, J. D.; Perry, D. L. *J. Inorg. Nucl. Chem.* **1973**, *35*, 3031 and references cited therein.
(8) Ortego, J. D.; Upalawanna, S.; Amanoilahi, S. *J. Inorg. Nucl. Chem.* **1979**, *41*, 593.
(9) Jagannathan, R.; Soundarajan, S. *J. Inorg. Nucl. Chem.* **1980**, *42*, 145.
(10) Ortego, J. D.; Seymour, M. *Polyhedron* **1982**, *1*, 21.
(11) Annibale, G.; Canovese, L.; Cattalini, L.; Natile, G.; Biagini-Cingi, M.; Manotti-Lanfredi, A. M.; Tiripicchio, A. *J. Chem. Soc., Dalton Trans.* **1981**, *2280*.
(12) Newkome, G. R.; Gupta, V. K.; Theriot, K. J.; Ewing, J. C.; Wicelinski, S. P.; Huie, W. R.; Fronczek, F. R.; Watkins, S. F. *Acta Crystallogr., Sect. C: Cryst. Struct. Commun.* **1984**, *C40*, 1352.
(13) Newkome, G. R.; Gupta, V. K.; Taylor, H. C. R.; Fronczek, F. R. *Organometallics* **1984**, *3*, 1549.

0020-1669/86/1325-1149$01.50/0